

Antineurodegenerative Labdane Diterpenoid Glycosides from the Twigs of *Pinus koraiensis*

Kyoung Jin Park, Zahra Khan, Lalita Subedi, Sun Yeou Kim, and Kang Ro Lee*



Cite This: <https://dx.doi.org/10.1021/acs.jnatprod.9b01158>



Read Online

ACCESS |



Metrics & More

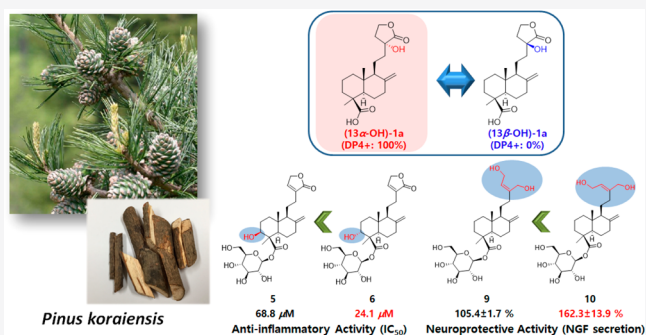


Article Recommendations



Supporting Information

ABSTRACT: Eleven new labdane-type diterpenoid glycosides, koraiensides A–K (1–11), together with two known analogues were isolated from the twigs of *Pinus koraiensis*. Their structures were elucidated via NMR, HRMS, and ECD data, DP4+ statistical analysis, and hydrolysis. The metabolites were tested for induction of nerve growth factor in C6 glioma cells to evaluate their potential neuroprotective activity. The compounds were measured for production of nitric oxide levels in lipopolysaccharide (LPS)-activated murine microglia BV2 cells to assess their anti-inflammatory activity. Compounds **10** and **13** showed NGF secretion inducing effects from C6 glioma cells ($162.3 \pm 13.9\%$ and $162.7 \pm 6.9\%$, respectively). Compound **6** showed an IC_{50} value of $24.1 \mu\text{M}$, implying significant inhibition of NO production.



Neurotrophic factors, such as nerve growth factor (NGF), play an important role in neuronal survival, development, and central network formation. NGF is produced by the brain cells in the nervous system for maintenance, migration, and differentiation of cells.¹ The loss of neurotrophic factors and production of neuroinflammation may contribute to the development of neurodegenerative disorders, including Parkinson's and Alzheimer's diseases.^{2,3} Uncontrolled activation of microglial cells can release pro-inflammatory cytokines such as NO due to excessive formation of inducible nitric oxide synthase (iNOS).⁴ Overproduction of NO can result in neuroinflammation, and it is vital to explore novel bioactive phytochemicals that can protect brain cells by initiating the production of NGF and mitigate neuroinflammation-targeting activated microglia.

Pinus koraiensis Siebold et Zucc., belonging to the Pinaceae family, is commonly known as “Korean pine” and mainly distributed in Korea, Russia, China, and Japan. Pine nuts, the seed crop of this tree, have been utilized as a supplementary health food and dessert all over the world.⁵ Phytochemical studies have reported various pharmacological activities associated with the components of pine nuts and pine cones of *P. koraiensis*. Fatty acids, peptides, and polysaccharides from the pine nuts were shown as the main components displaying antifatigue, antiaging, anti-inflammatory, antioxidant, and hepatoprotective effects.^{6–8} Further, cytotoxic and angiogenesis inhibitory diterpenoids,^{5,9} antioxidant polysaccharides,¹⁰ and antitumor, antioxidant, and immunoregulatory polyphenols^{11,12} were identified from the pine cones of *P. koraiensis*.

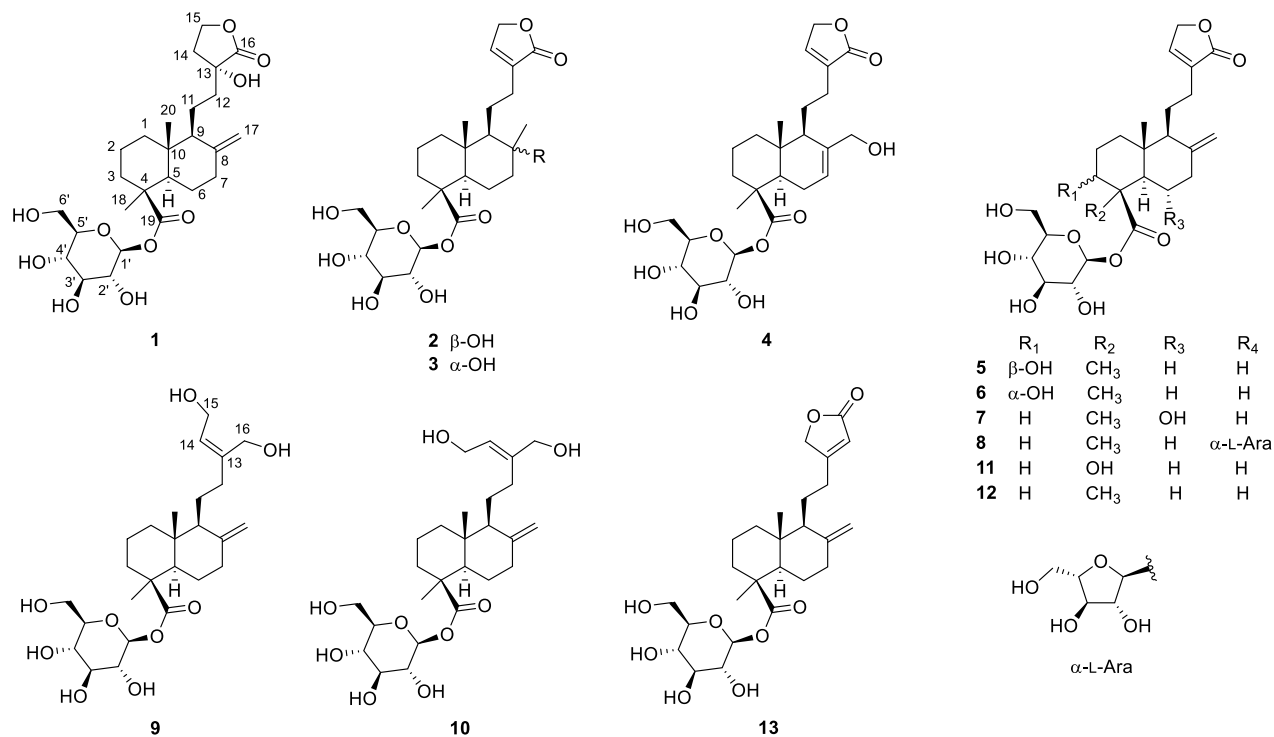
In ongoing research on bioactive substances from Korean native plants, the EtOAc layer of the MeOH extract from *P. koraiensis* twigs showed that the solvent layer induces NGF release in C6 glioma cells (EtOAc-soluble layer, $153.8 \pm 15.2\%$; positive control, 6-shogaol, $150.8 \pm 8.9\%$). In contrast, the *n*-hexane-soluble layer ($57.5 \pm 11.4\%$), CHCl_3 -soluble layer ($45.8 \pm 11.5\%$), and *n*-BuOH-soluble layer ($150.8 \pm 2.8\%$) showed weak or similar activities when compared with the positive control. From the active EtOAc layer, 11 new diterpenoid glycosides (1–10), including a norditerpenoid glycoside (11), together with the known compounds 12 and 13 were isolated and characterized. The structures of the new compounds were elucidated based on the analysis of various NMR (^1H and ^{13}C NMR, COSY, HSQC, HMBC, and NOESY), HRMS, and ECD data, DP4+ computation, and hydrolysis. The known analogues 12 and 13 were characterized by comparing the observed spectra with reported data. The purified compounds (2–13) were evaluated for their neuroprotective and anti-inflammatory activities.

RESULTS AND DISCUSSION

The 80% MeOH extract of the twigs of *P. koraiensis* was sequentially fractionated using *n*-hexane, CHCl_3 , EtOAc, and

Received: November 20, 2019

Chart 1



n-BuOH. Such fractions were assessed for their neuroprotective activity. The EtOAc-soluble fraction displayed considerable NGF secretion effect and thus was subjected to repeated chromatographic purification. As a result, 11 new diterpenoid glycosides (1–11) and two known analogues (12 and 13) were purified and identified.

Koraienside A (1) was obtained as a colorless gum, and its molecular formula was established as C₂₆H₄₀O₁₀ based on the [M + Na]⁺ ion in the HRESIMS data. The 1D NMR spectroscopic data of 1 revealed the characteristic signals for two tertiary methyls [δ_C 29.5 (C-18) and 13.9 (C-20)]; δ_H 1.19 (3H, s, Me-18) and 0.58 (3H, s, Me-20)], an exocyclic methylene [δ_C 107.3 (C-17); δ_H 4.81 (1H, brs, H-17a) and 4.51 (1H, brs, H-17b)], a γ -lactone group [δ_C 178.9 (C-16), 80.3 (C-15), 78.2 (C-13), and 42.9 (C-14)]; δ_H 4.11 (2H, overlap, H-15), 2.59 (1H, dd, J = 17.2, 12.6 Hz, H-14a), and 2.37 (1H, dd, J = 17.2, 9.7 Hz, H-14b)], and a glucopyranosyl moiety [δ_C 95.7 (C-1'), 78.9 (C-5'), 78.6 (C-3'), 74.2 (C-2'), 71.3 (C-4'), and 62.6 (C-6'); δ_H 5.37 (1H, d, J = 8.2 Hz, H-1'), 3.75 (1H, dd, J = 11.9, 1.8 Hz, H-6'a), 3.62 (1H, dd, J = 11.9, 4.6 Hz, H-6'b), and 3.33–3.28 (4H, m, H-2',3',4',5')], indicating that compound 1 is a labdane-type diterpenoid glycoside (Tables 1 and 2).^{13,14} These data were similar to those of adenanthoside C (12),¹⁵ except for the resonances of an oxygenated carbon (δ_C 78.2) and a methylene group [δ_C 42.9; δ_H 2.59 (1H, dd, J = 17.2, 12.6 Hz) and 2.37 (1H, dd, J = 17.2, 9.7 Hz)], instead of a $\Delta^{13(14)}$ olefinic functionality [δ_C 146.2; δ_H 7.35 (1H, brs) and δ_C 133.3] in 12. Analysis of the COSY, HSQC, and HMBC spectra corroborated the 2D structure of 1 (Figure 1A). The location of an oxygenated carbon and a glucosyl unit was deduced to be at C-13 and C-19 via the HMBC correlations from H₂-14 and H₂-15 to C-13 and from H-1' to C-19, respectively. The characteristic coupling constant of the anomeric proton (J = 8.2 Hz) showed that the glucosyl moiety had a β -anomeric

configuration.¹⁶ The NOESY correlations of H-5/H-9 and H₃-18, and H₂-11/H₃-20 indicated a *trans*-fused A/B ring junction (Figure 1A). The orientation of the hydroxy group at C-13 was verified based on a DP4+ computational analysis.¹⁷ The calculated ¹H and ¹³C NMR data of (13 α -OH)-1a and (13 β -OH)-1a were compared with the experimental values of 1a, the hydrolysate of 1, using DP4+ computational analysis. The statistical results showed that (13 α -OH)-1a is structurally coincident to 1a with an α -oriented OH group at C-13 (Figure 1B, S123, and S124, Supporting Information). For determination of the absolute configuration of 1, the experimental ECD data of 1a was compared with the calculated ECD data of the two plausible enantiomers of 1a, (4*S*,5*R*,9*S*,10*R*,13*R*)-1a and (4*R*,5*S*,9*R*,10*S*,13*S*)-1a. The experimental ECD spectrum of 1a exhibited a positive Cotton effect at 222 nm, which was identical to the calculated data for (4*S*,5*R*,9*S*,10*R*,13*R*)-1a (Figure 1C), thus confirming the (13*R*) absolute configuration of 1.

Enzymatic hydrolysis of 1 with β -glucosidase gave the aglycone (1a) and a glucosyl unit. The D-configuration of the glucosyl moiety was established through chiral derivatization and GC/MS analysis.¹⁸ Based on HRESIMS data, the molecular formula of 1a was confirmed as C₂₀H₃₀O₅ and its 1D and 2D NMR spectra showed the absence of a glucosyl unit when compared with those of 1 (Figures S1 and S2 and Tables S6 and S7, Supporting Information).¹⁹ Thus, 1a was identified as 13 α -hydroxy-8(17)-labden-(15→16)-lacton-19-oic acid, and the structure of 1 as β -D-glucopyranosyl 13 α -hydroxy-8(17)-labden-(15→16)-lacton-19-oate.

Koraienside B (2), a colorless gum, has a molecular formula of C₂₆H₄₀O₁₀. Its NMR data resembled those of 12,¹⁵ but oxygenated carbon (δ_C 73.6) and tertiary methyl [δ_C 31.0; δ_H 1.12 (3H, s)] signals were present instead of the exocyclic double-bond signals [δ_C 149.1 and δ_C 107.2; δ_H 4.91 (1H, s) and 4.66 (1H, s)] at C-8 and C-17 in 12 (Tables 1 and 2). The

Table 1. ¹H NMR [ppm, mult., (J in Hz)] Spectroscopic Data of Compounds 1–11 in Methanol-d₄

pos	1	2	3	4	5	6	7	8	9	10	11
1 α	1.10, brt (13.4)	0.91, td (13.2, 3.8)	1.05, td (13.2, 3.7)	0.93, td (13.3, 3.8)	1.27, td (13.0, 3.7)	1.43, dd (9.2, 3.3)	1.11, td (12.8, 4.0)	1.05, overlap	1.16, td (12.7, 3.3)	1.00, overlap	1.09, td (13.9, 3.9)
1 β	1.83, overlap	1.72, overlap	1.81, brd (12.5)	1.85, m	1.92, dt (13.0, 3.4)	1.43, dd (9.2, 3.3)	1.82, overlap	1.80, brd (12.7)	1.89, brd (12.7)	1.73, brd (13.0)	1.78, brd (13.9)
2 α	1.46, brd (13.4)	1.37, overlap	1.47, m	1.39, overlap	1.77, m	1.53, m	1.49, overlap	1.44, m	1.52, overlap	1.41, overlap	1.58, overlap
2 β	1.90, m	1.93, qt (13.8, 3.3)	2.01, dt (13.8, 3.3)	1.89, dt (13.3, 3.1)	2.31, dd (13.0, 3.4)	2.08, dd (9.7, 2.1)	1.85, overlap	1.89, overlap	1.96, overlap	1.84, overlap	1.93, dt (14.3, 3.9)
3 α	2.16, brd (13.4)	2.11, overlap	2.21, brd (13.4)	2.13, m	3.22, dd (12.2, 4.4)	3.94, brt (2.8)	2.19, dd (13.4, 1.3)	2.14, brd (13.2)	2.23, brd (13.2)	2.09, overlap	2.25, brd (12.9)
3 β	1.06, td (13.4, 3.4)	1.02, td (13.8, 4.1)	1.10, td (13.7, 4.4)	1.01, td (13.3, 3.7)	1.38, dd (12.7, 2.7)	1.72, dd (12.3, 2.8)	1.17, td (13.4, 3.9)	1.05, overlap	1.12, td (13.2, 3.6)	1.00, overlap	1.30, td (13.4, 4.4)
5	1.35, m	1.13, overlap	1.24, dd (11.9, 2.7)	1.41, overlap	1.38, dd (12.7, 2.7)	1.72, dd (12.3, 2.8)	1.37, d (10.5)	1.34, m	1.42, brd (9.1)	1.29, m	1.54, dd (13.1, 2.6)
6 α	1.98, m	2.11, overlap	1.96, m	2.55, m	2.04, m	1.87, m	4.36, td (10.5, 4.8)	1.98, m	2.05, brd (8.2)	2.07, overlap	2.11, m
6 β	1.88, overlap	1.72, overlap	1.91, m	2.19, m	1.79, m	1.80, m	1.87, overlap	1.87, overlap	1.95, overlap	1.93, overlap	1.62, dd (13.1, 3.9)
7 α	1.88, overlap	1.37, overlap	1.43, dd (12.3, 3.9)	5.69, m	1.98, td (12.9, 4.1)	1.85, m	2.07, brt (12.1)	1.87, overlap	1.95, overlap	1.82, m	1.90, m
7 β	2.35, m	1.72, overlap	1.86, dt (12.3, 3.2)	2.45, m	2.45, m	2.33, dd (8.7, 2.5)	2.66, dd (12.1, 4.8)	2.37, m	2.43, m	2.32, dd (8.5, 2.6)	2.39, m
9	1.56, m	0.79, dd (4.2, 2.5)	1.16, brt (3.9)	1.84, m	1.66, overlap	1.62, brd (11.0)	1.71, brd (10.8)	1.61, overlap	1.68, brd (10.7)	1.52, overlap	1.66, brd (10.7)
11a	1.62, m	1.65, m	1.67, m	1.66, m	1.80, m	1.68, dd (15.1, 7.2)	1.79, overlap	1.73, m	1.72, m	1.52, overlap	1.73, m
11b	1.41, m	1.47, m	1.56, m	1.42, overlap	1.66, overlap	1.52, m	1.61, m	1.58, m	1.52, overlap	1.38, overlap	1.58, overlap
12a	1.82, overlap	2.26, m	2.47, m	2.51, m	2.41, m	2.29, m	2.42, m	2.34, m	2.35, m	2.09, overlap	2.35, m
12b	1.36, m	2.21, m	2.30, m	2.23, m	2.13, m	2.02, dt (15.1, 7.7)	2.13, ddd (15.2, 8.2, 7.1)	2.04, dt (15.0, 7.4)	1.94, overlap	1.93, overlap	2.06, dt (15.2, 7.7)
14a	2.59, dd (17.2, 12.6)	7.31, brt (1.3)	7.38, brt (1.3)	7.28, brt (1.3)	7.36, brt (1.4)	7.23, brt (1.3)	7.34, brt (1.4)	7.28, brt (1.7)	5.47, t (6.6)	5.50, t (6.6)	7.29, brt (1.4)
14b	2.37, dd (17.2, 9.7)										
15	4.11, overlap	4.77, overlap	4.83, overlap	4.74, overlap	4.84, overlap	4.72, overlap	4.83, overlap	4.76, overlap	4.16, d (6.6)	3.89, brs	4.77, overlap
16a									4.13, d (12.4)	4.02, dd (12.6, 6.8)	
16b									4.09, d (12.4)	3.96, dd (12.6, 6.8)	
17a	4.81, brs	1.12, s	1.18, s	4.09, d (12.1)	4.92, brs	4.79, brs	4.97, brs	4.84, brs	4.88, brs	4.79, brs	4.86, brs
17b	4.51, brs			3.86, d (12.1)	4.68, brs	4.54, brs	4.73, brs	4.58, brs	4.60, brs	4.53, brs	4.61, brs
18	1.19, s	1.20, s	1.27, s	1.16, s	1.46, s	1.20, s	1.50, s	1.20, s	1.26, s	1.14, s	
20	0.58, s	0.82, s	0.78, s	0.63, s	0.70, s	0.53, s	0.61, s	0.57, s	0.64, s	0.50, s	0.57, s
1'	5.37, d (8.2)	5.40, d (8.2)	5.47, d (8.2)	5.38, d (8.2)	5.49, d (8.2)	5.33, d (8.2)	5.44, d (8.2)	5.36, d (8.2)	5.44, d (8.2)	5.32, d (8.2)	5.36, d (8.2)
2'	3.28, m	3.30, m	3.36, m	3.26, m	3.88, m	3.24, m	3.36, m	3.28, m	3.35, m	3.23, m	3.33, m
3'	3.33, m	3.34, m	3.41, m	3.30, m	3.41, m	3.28, m	3.40, m	3.33, m	3.40, m	3.28, m	3.35, m
4'	3.30, m	3.33, m	3.38, m	3.28, m	3.40, m	3.21, m	3.36, m	3.28, m	3.37, m	3.26, m	3.32, m
5'	32.9, m	3.28, m	3.38, m	3.26, m	3.36, m	3.23, m	3.36, m	3.45, ddd (9.4, 5.7, 2.4)	3.36, m	3.24, m	3.30, m

C

Table 1. continued

pos	1	2	3	4	5	6	7	8	9	10	11
6'a	3.75, dd (11.9, 1.8)	3.73, dd (12.0, 2.3)	3.84, dd (11.9, 1.9)	3.72, dd (12.0, 1.9)	3.81, dd (11.9, 2.3)	3.70, dd (11.9, 1.9)	3.81, brd (11.9)	3.89, dd (11.1, 3.0)	3.83, dd (11.6, 1.5)	3.71, dd (11.9, 1.8)	3.74, dd (11.9, 2.0)
6'b	3.62, dd (11.9, 4.6)	3.63, dd (12.0, 4.7)	3.70, dd (11.9, 4.5)	3.59, dd (12.0, 4.6)	3.70, dd (11.9, 4.8)	3.57, dd (11.9, 4.7)	3.67, dd (11.9, 4.5)	3.52, dd (11.1, 5.7)	3.69, dd (11.6, 4.2)	3.57, dd (11.9, 4.6)	3.62, dd (11.9, 4.6)
1"								4.84, d (2.0)			
2"								3.91, overlap			
3"								3.76, dd (5.8, 2.2)			
4"								3.90, overlap			
5"a								3.68, dd (11.9, 3.3)			
5"b								3.58, dd (11.9, 5.1)			

HMBC correlations of H-17/C-7, C-8, and C-9 indicated that the OH group is located at C-8 (Figure 2). The relative configuration of C-8 was determined through the NOESY cross-peak of H-9/H-17, indicating the hydroxy group at C-8 is β -orientated (Figure 3). The configuration of the glucosyl unit was confirmed by the same method as described for 1. Therefore, the structure of compound 2 was assigned as β -D-glucopyranosyl 8 β -hydroxy-labd-13-en-(15 \rightarrow 16)-lacton-19-oate.

Koraienside C (3) was purified as a colorless gum and had the molecular formula $C_{26}H_{40}O_{10}$, the same as 2 from the HRESIMS data. The 1D NMR spectroscopic data of 3 were close to those of 2, with the main difference in the carbon chemical shift of the 17-methyl group (δ_C 23.6, 3; δ_C 31.0, 2), suggesting that 3 was an epimer of 2 (Tables 1 and 2). The 2D NMR spectra were analyzed to corroborate the 2D structure of 3, which confirmed it to be identical to 2. Based on the NOESY correlation between H-11 and H-17, the hydroxy group at C-8 was assigned an α -orientation (Figure 3). Thus, the structure of 3 was elucidated as β -D-glucopyranosyl 8 α -hydroxylabd-13-en-(15 \rightarrow 16)-lacton-19-oate.

The molecular formula of koraienside D (4), a colorless gum, was defined as $C_{26}H_{38}O_{10}$ from the HRESIMS data. Comparison of the NMR spectra with data of 12¹⁵ displayed the presence of a C-17 oxygenated methylene [δ_C 66.2; δ_H 4.09 (1H, d, $J = 12.1$ Hz) and 3.86 (1H, d, $J = 12.1$ Hz)] and $\Delta^{7(8)}$ double-bond signals [δ_C 126.8; δ_H 5.69 (m) and δ_C 138.9] in 4 instead of exocyclic double-bond signals [δ_C 149.1 and δ_C 107.2; δ_H 4.91 (1H, s) and 4.66 (1H, s)] for C-8/C-17 in 12 (Tables 1 and 2). In the HMBC spectrum, the correlations of H-17/C-7, C-8, and C-9 corroborated the oxygenated methylene group at C-17 and the $\Delta^{7(8)}$ olefinic functionality (Figure 2). The NOESY data of 4 showed correlations of H-5/H-9, H-5/H-18, and H-11/H-20, which proved the relative configuration of 4 (Figure 3). The sugar analysis of 4 was performed as for 1. Accordingly, compound 4 was defined as β -D-glucopyranosyl 17-hydroxy-labda-7,13-diene-(15 \rightarrow 16)-lacton-19-oate.

Koraienside E (5) gave a molecular formula of $C_{26}H_{38}O_{10}$ deduced from the molecular ion at m/z 533.2366 [$M + Na$]⁺ (calcd for $C_{26}H_{38}O_{10}Na$, 533.2363) in the HRESIMS data. The ¹H and ¹³C NMR spectra of 5 showed similarity with those of adenanthoside C (12) (Tables 1 and 2).¹⁵ The main distinction was that 5 has an oxygenated methine [δ_C 79.3; δ_H 3.22 (1H, dd, $J = 12.2, 4.4$ Hz)], replacing a methylene in 12. The hydroxy group at C-3 was verified based on the HMBC correlation of H-18/C-3 and the COSY correlation of H-2/H-3 (Figure 2). The β -orientation of the hydroxy group at C-3 was corroborated through the J value of H-3 ($J_{H-2\alpha/H-3} = 4.4$ Hz and $J_{H-2\beta/H-3} = 12.2$ Hz) confirmed in the ¹H NMR data and further identified by the cross-peak of H-3/H-5 in the NOESY data (Figure 3). Therefore, the structure of compound 5 was assigned as β -D-glucopyranosyl 3 β -hydroxylabda-8(17),13-diene-(15 \rightarrow 16)-lacton-19-oate.

Koraienside F (6) was purified as a colorless gum with the same molecular formula, $C_{26}H_{38}O_{10}$, as 5. The NMR spectroscopic data of 6 were highly similar to the data of 5, except for the C-3 resonances of 6 [δ_C 71.4; δ_H 3.94 (1H, brt, $J = 2.8$ Hz)], compared with those of 5 [δ_C 79.3; δ_H 3.22 (1H, dd, $J = 12.2, 4.4$ Hz)], indicating that 6 is an epimer of 5 (Tables 1 and 2). The 2D structure of 6 was defined via analysis of the NMR data and confirmed to be the same as 5. The coupling constants of H-3 ($J_{H-2\alpha/H-3} = 2.8$ Hz and $J_{H-2\beta/H-3}$

Table 2. ^{13}C NMR Spectroscopic Data of Compounds 1–11 in Methanol- d_4

pos	1	2	3	4	5	6	7	8	9	10	11
1	40.5	40.9	41.3	40.5	38.9	33.6	40.7	40.5	39.0	38.9	39.5
2	21.3	20.1	20.3	20.8	29.4	28.1	20.9	21.2	19.7	19.7	21.3
3	39.3	39.2	39.0	39.3	79.3	71.4	41.0	39.4	37.8	37.8	39.2
4	45.9	45.4	45.4	45.4	51.3	49.8	46.7	45.8	44.3	44.3	76.6
5	58.0	58.4	58.4	52.9	57.1	50.1	62.6	57.9	56.4	56.4	58.0
6	27.4	21.1	23.2	25.6	27.1	27.0	72.7	27.5	25.9	26.3	25.7
7	40.0	43.3	45.3	126.8	39.6	40.0	49.8	39.9	38.4	38.4	39.4
8	149.4	73.6	74.8	138.9	148.7	149.3	146.4	149.2	148.1	148.1	148.9
9	57.9	59.6	61.8	51.7	57.0	56.7	56.4	57.1	55.5	55.3	57.2
10	41.9	40.8	41.0	38.3	41.1	41.4	41.5	41.7	40.1	40.1	41.9
11	19.2	24.8	24.9	26.4	23.4	23.1	23.5	23.2	22.1	22.3	23.3
12	38.3	29.8	29.6	27.6	25.6	25.5	25.6	25.6	33.5	26.3	25.6
13	78.2	134.9	135.2	134.8	134.8	134.8	134.8	134.9	141.9	141.5	134.8
14	42.9	147.7	147.6	148.1	147.8	147.8	147.8	147.7	126.1	124.4	147.8
15	80.3	72.2	72.2	72.2	72.2	72.2	72.2	72.2	57.3	64.8	72.2
16	178.9	177.1	177.3	177.1	177.1	177.1	177.0	177.1	58.6	57.8	177.1
17	107.3	31.0	23.6	66.2	107.8	107.3	108.9	107.4	105.6	105.6	107.9
18	29.5	29.3	29.3	29.2	24.6	25.0	32.8	29.3	27.9	27.9	
19	177.7	178.0	177.7	177.6	176.3	177.3	177.9	177.7	176.2	176.2	174.2
20	13.9	14.2	14.2	13.8	13.7	13.7	15.4	14.0	12.4	12.4	13.6
1'	95.7	95.6	95.7	95.7	95.8	95.6	96.0	95.5	94.1	94.1	96.4
2'	74.2	74.3	74.3	74.2	74.1	71.4	74.1	74.1	72.7	72.7	74.0
3'	78.6	78.6	78.6	78.6	78.5	78.6	78.3	78.5	77.1	77.1	78.1
4'	71.3	71.1	71.3	71.3	71.3	74.2	71.4	71.9	69.8	69.8	71.4
5'	78.9	78.7	78.8	78.9	78.8	78.9	78.9	77.5	77.3	77.3	78.8
6'	62.6	62.4	62.7	62.6	62.6	62.7	62.6	68.0	61.1	61.1	62.7
1''								109.9			
2''								83.1			
3''								79.0			
4''								86.0			
5''								63.1			

= 2.8 Hz) in the ^1H NMR spectrum of **6** and the NOESY correlations of H-3/H-18 and H-5/H-18 were confirmed, but no cross-peak appeared between H-3 and H-5 (Figure 3). This evidence revealed that the OH group at C-3 is α oriented. Consequently, the structure of **6** was elucidated as β -D-glucopyranosyl 3 α -hydroxylabda-8(17),13-diene-(15 \rightarrow 16)-lacton-19-oate.

Koraienside G (**7**) was obtained as a colorless gum, and its molecular formula was defined as identical to that of **6** ($\text{C}_{26}\text{H}_{38}\text{O}_{10}$) based on the HRESIMS data. The NMR data of **7** showed that this molecule is closely similar to **6**, with the main differences in resonances at C-3 (δ_{C} 41.0, **7**; δ_{C} 71.4, **6**) and C-6 (δ_{C} 72.7, **7**; δ_{C} 27.0, **6**), implying that the OH functionality at C-3 in **6** is shifted to C-6 in **7** (Tables 1 and 2). The location of the hydroxy group was corroborated to be at C-6 based on signals of H-5/H-6 and H-6/H-7 in the COSY data (Figure 2). The NOESY cross-peak between H-6 and H₃₋₂₀ suggested that the hydroxy group at C-6 is α oriented (Figure 3). Thus, the structure of compound **7** was assigned as β -D-glucopyranosyl 6 α -hydroxylabda-8(17),13-diene-(15 \rightarrow 16)-lacton-19-oate.

The molecular formula of koraienside H (**8**) was confirmed as $\text{C}_{31}\text{H}_{46}\text{O}_{13}$ based on the HRESIMS ion at m/z 649.2832 [$\text{M} + \text{Na}$] $^+$ (calcd for $\text{C}_{31}\text{H}_{46}\text{O}_{13}\text{Na}$, 649.2836). The 1D NMR spectra of **8** was comparable with the data of **12**,¹⁵ except for the additional arabinofuranose signals [δ_{C} 109.9 (C-1''), 86.0 (C-4''), 83.1 (C-2''), 79.0 (C-3''), and 63.1 (C-5''); δ_{H} 4.84 (1H, d, $J = 2.0$ Hz, H-1''), 3.91 (1H, overlap, H-2''), 3.90 (1H,

overlap, H-4''), 3.76 (1H, dd, $J = 5.8, 2.2$ Hz, H-3''), 3.68 (1H, dd, $J = 11.9, 3.3$ Hz, H-5''a), and 3.58 (1H, dd, $J = 11.9, 5.1$ Hz, H-5''b)] and a deshielded resonance of C-6' (δ_{C} 68.0, **8**; δ_{C} 62.5, **12**) (Tables 1 and 2). The small coupling constant of H-1'' ($J = 2.0$ Hz) in **8** verified an α -arabinofuranosyl moiety.²⁰ The analysis of additional 2D NMR spectra confirmed the 2D structure of **8** (Figure 2). The HMBC data confirmed that the position of the α -arabinofuranosyl unit is C-6' based on the correlation of H-1''/C-6'. Sugar analysis of **8** was performed using the same method as **1**, and L-arabinofuranose and D-glucopyranose were confirmed. However, the acid hydrolysis led to the generation of labda-8,13-dien-16,15-olid-19-oic acid (**8b**) not pinusolidic acid (**8a**) (Figure S1, Supporting Information).¹⁹ Thus, the enzymatic hydrolysis of **8** was performed to give the aglycone pinusolidic acid (**8a**). The structure of **8a** was confirmed by comparison with the reported ^1H NMR, MS, and ECD spectra.^{19,21} Therefore, the structure of compound **8** was defined as α -L-arabinofuranosyl-(1 \rightarrow 6)-O- β -D-glucopyranosyl labda-8(17),13-diene-(15 \rightarrow 16)-lacton-19-oate.

Koraienside I (**9**) was obtained as a colorless gum and identified as $\text{C}_{26}\text{H}_{42}\text{O}_9$, showing a positive-ion signal [$\text{M} + \text{Na}$] $^+$ at m/z 521.2725 based on the HRESIMS data. Assignments of the 1D NMR data of **9** indicated characteristic resonances of a labdane diterpenoid glycoside (Tables 1 and 2).^{13,14} The main differences in NMR data of **9** compared with those of **12**¹⁵ were attributed to the presence of two oxygenated methylenes [δ_{C} 57.3; δ_{H} 4.16 (2H, d, $J = 6.6$

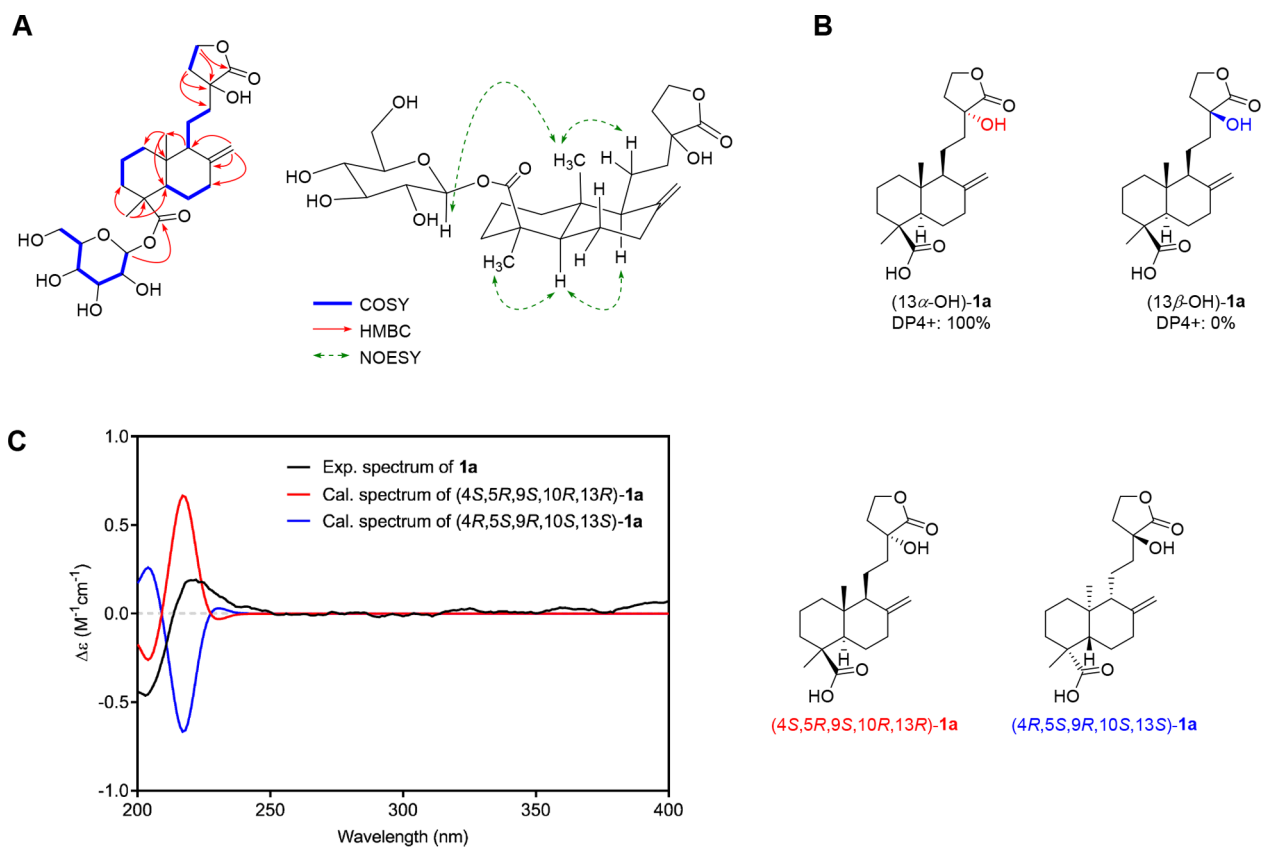


Figure 1. Structural elucidation of **1**. (A) Key COSY, HMBC, and NOESY correlations. (B) Results of DP4+ analysis for (13 α -OH)-**1a** and (13 β -OH)-**1a**. (C) Comparison of the experimental and calculated ECD spectra of **1a**.

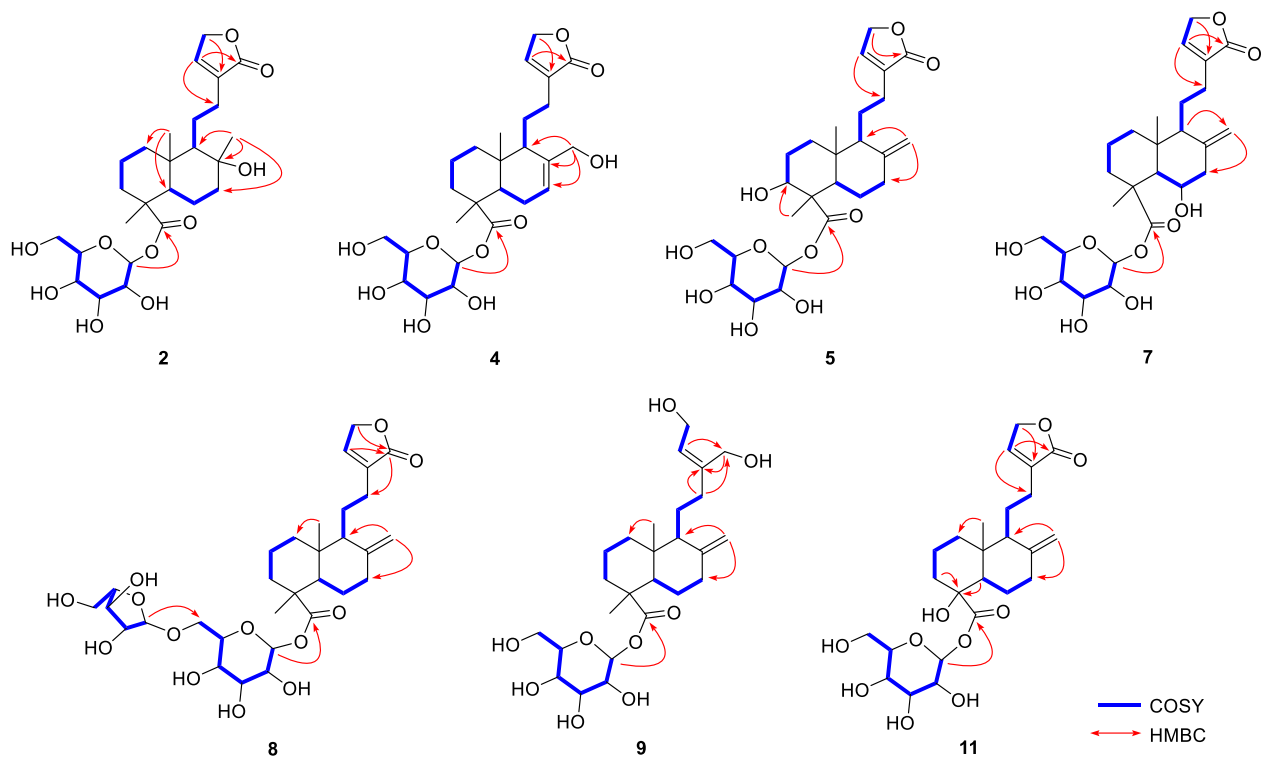


Figure 2. Key COSY and HMBC correlations of **2–5**, **7–9**, and **11**.

Hz) and δ_C 58.6; δ_H 4.13 (1H, d, $J = 12.4$ Hz) and 4.09 (1H, d, $J = 12.4$ Hz)] in **9**, instead of the α,β -unsaturated lactone signals [δ_C 72.1; δ_H 4.84 (2H, overlap) and δ_C 177.0] in **12**.

The 2D structure of **9** was established via full NMR assignments and confirmed to be identical with the *ent*-labdane diterpenoid andrographatoside, which was isolated

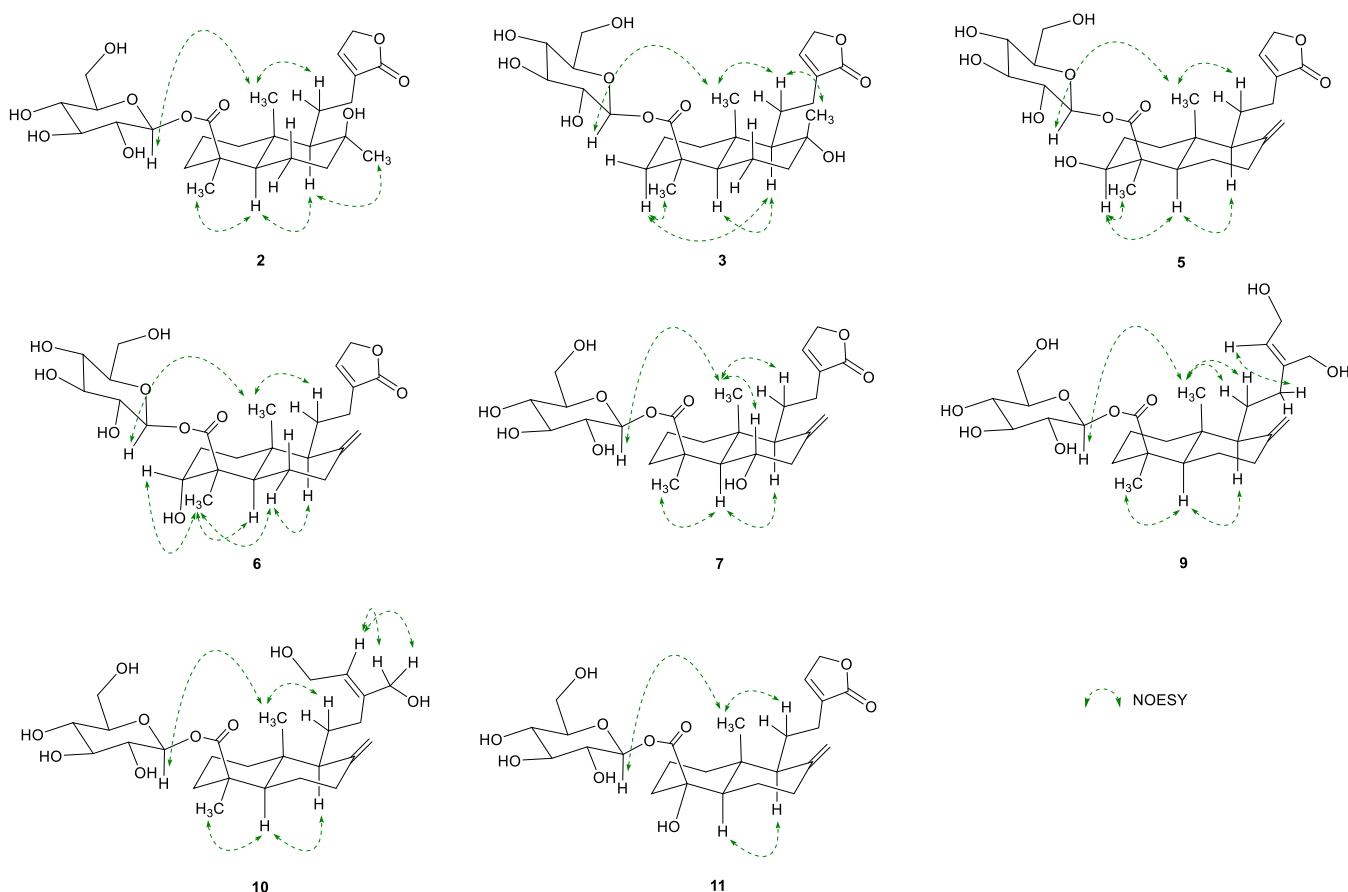


Figure 3. Key NOESY correlations of 2, 3, 5–7, and 9–11.

from *Andrographis paniculata*.²² The geometry of the $\Delta^{13(14)}$ double bond was corroborated through NOESY correlation of H-12/H-14, which implied a *Z*-geometry (Figure 3). The experimental ECD spectrum showed that **9** has the same absolute configuration as **1**. Consequently, compound **9** was established as β -D-glucopyranosyl labda-8(17),13*Z*-diene-15,16-diol-19-oate.

Koraienside J (**10**) had the same molecular formula, $C_{26}H_{42}O_9$, as **9**. The NMR assignments of **10** also exhibited close similarities with those of **9**, with significant differences in chemical shifts at C-12 (δ_C 26.3, **10**; δ_C 33.5, **9**), C-14 (δ_C 124.4, **10**; δ_C 126.1, **9**), and C-15 (δ_C 64.8, **10**; δ_C 57.3, **9**), suggesting that **10** is a geometric isomer of **9** (Tables 1 and 2). The NOESY cross-peak of H-14/H-16 indicated the *E*-geometry of the $\Delta^{13(14)}$ olefinic bond (Figure 3). Enzymatic hydrolysis of **10** yielded the aglycone **10a** and D-glucose. The sugar moiety was analyzed using the same method as **1**. The structure of **10a** was implied through HRESIMS data analysis. Thus, the structure of compound **10** was assigned as β -D-glucopyranosyl labda-8(17),13*E*-diene-15,16-diol-19-oate.

Koraienside K (**11**) was purified as a colorless gum. Its molecular formula was determined as $C_{25}H_{36}O_{10}$ by HRESIMS, displaying a positive-ion peak $[M + Na]^+$ at m/z 519.2208 (calcd for $C_{25}H_{36}O_{10}Na$, 519.2206). Comparison of the 1D NMR spectra indicated that **11** has an oxygenated tertiary carbon (δ_C 76.6) instead of a methyl group [δ_C 29.4; δ_H 1.27 (3H, s)] and a quaternary carbon (δ_C 45.7) in **12**.¹⁵ The HMBC correlations of H-3/C-4 and H-5/C-4 verified that the hydroxy group is positioned at C-4 (Figure 2). Based on 2D NMR and HRESIMS data, the skeleton of a norditerpenoid

glucoside was established for **11** (Figure 2). The presence of rare 18-norditerpenoids in natural products was additionally confirmed through previous reports.^{23–25} The relative configuration of C-4 in **1–10** was established by NOESY correlations of H₃-20/H-1' and H-5/H₃-18 (Figures 1A and 3). The same NOESY correlation of H₃-20/H-1' was observed in **11**, indicating that C-19 was in a β -axial position as in **1–10** (Figure 3). This initial assignment was supported by the calculated interproton distance between H₃-20 and H-1' in two C-4 epimers (**11r** and **11s**). The Boltzmann-averaged interproton distances between H₃-20 and H-1' were 3.94 and 6.83 Å in **11r** and **11s**, respectively (Figures S125 and S126, Supporting Information). Since the maximum distance between two protons that allows for the NOESY cross-peak observation is ~ 5 Å,²⁶ only **11r** could be the possible epimer for **11**. Hence, the structure of **11** was defined as β -D-glucopyranosyl 18-norlabda-8(17),13-diene-(15→16)-lacton-19-oate.

The other two known analogues were characterized as adenanthoside C (**12**)¹⁵ and β -D-glucopyranosyl (4*S*,5*R*,9*S*,10*R*)-labda-8(17),13-dien-15,16-olid-19-oate (**13**)¹⁹ by comparing the experimental spectra reported data.

In order to evaluate the neuroprotective effects of compounds **2–13**, their efficacy on NGF release in C6 cells was tested (Table 3). Treatment with **10** and **13** considerably induced NGF secretion, with values of NGF stimulated at $162.3 \pm 13.9\%$ and $162.7 \pm 6.9\%$, respectively (6-shogaol, a positive control, $150.9 \pm 8.9\%$), without any cytotoxicity toward normal cells at a 20 μ M concentration. Interestingly, despite the structural similarity, **10** exhibited considerable

Table 3. Effects of Selected Compounds (2–13) on NGF Secretion in C6 Cells

compound	NGF secretion ^a (%)	cell viability ^b (%)
2	106.1 ± 1.3	94.2 ± 2.6
3	84.5 ± 0.2	111.2 ± 9.1
4	119.4 ± 5.1	101.6 ± 2.3
5	134.7 ± 3.9	98.3 ± 7.9
6	106.6 ± 4.0	92.8 ± 5.1
7	128.7 ± 8.0	101.4 ± 7.5
8	112.5 ± 1.3	93.3 ± 3.7
9	105.4 ± 1.7	86.5 ± 0.2
10	162.3 ± 13.9	104.0 ± 0.1
11	98.6 ± 1.7	76.0 ± 6.9
12	142.4 ± 6.7	101.0 ± 4.8
13	162.7 ± 6.9	105.0 ± 3.8
6-shogaol ^c	150.9 ± 8.9	108.8 ± 0.6

^aC6 cells were treated with 20 μ M of each compound. After 24 h, the content of NGF secreted into the C6-conditioned medium was measured by ELISA. The level of secreted NGF is expressed as the percentage of the untreated control (set as 100%). ^bThe cell viability after treatment with 20 μ M of each compound was determined by an MTT assay and is expressed as a percentage (%). Results are the means of three independent experiments, and the data are expressed as means \pm SD. ^cPositive control substance.

activity (162.3 \pm 13.9%), but the activity of 9, the geometric isomer, was relatively weak (105.4 \pm 1.7%).

The potential antineuroinflammatory activity of compounds 2–13 was tested by measuring NO levels produced in the BV2 cell line (Table 4). Compound 6 strongly inhibited NO

Table 4. Inhibitory Effects of Selected Compounds (2–13) on NO Production Induced by LPS in BV2 Cells

compound	IC ₅₀ (μ M) ^a	cell viability (%) ^b
2	49.2	89.6 \pm 4.1
3	402.0	70.4 \pm 5.2
4	93.2	87.7 \pm 3.1
5	68.8	91.3 \pm 2.5
6	24.1	77.5 \pm 7.7
7	35.7	99.7 \pm 4.1
8	>500	69.3 \pm 1.0
9	151.5	132.6 \pm 3.5
10	65.4	134.6 \pm 4.6
11	51.6	80.7 \pm 5.8
12	65.8	92.1 \pm 3.3
13	54.1	107.2 \pm 4.5
L-NMMA ^c	28.8	99.2 \pm 1.0

^aThe IC₅₀ value of each compound was defined as the concentration (μ M) that caused 50% inhibition of NO production in LPS-activated BV2 cells. ^bThe cell viability after treatment with 20 μ M of each compound was measured using the MTT assay and is expressed as a percentage (%). Results are the means of three independent experiments, and data are expressed as the means \pm SD. ^cPositive control substance.

production (IC₅₀ 24.1 μ M) and was comparable to L-NMMA, a positive control (IC₅₀ 28.8 μ M), with insignificant cytotoxicity at 20 μ M. Even if compounds 5 and 6 have similar structures, they showed different inhibitory effects on NO production (IC₅₀ 68.8 μ M, 5; IC₅₀ 24.1 μ M, 6), indicating that the orientation of the hydroxy functionality at C-3 may

play a substantial role in inhibition of inflammation. Compound 7 exhibited moderate activity (IC₅₀ 35.7 μ M).

In summary, 11 new labdane-type diterpenoid glycosides (1–11) were isolated from the twigs of *P. koraiensis*, together with two known analogues, 12 and 13. The aglycones 1a–6a and 9a were identified as new diterpenoid acids via NMR and HRMS data analysis. Among the isolates, compounds 10 and 13 showed neuroprotective effects, and compound 6 exhibited antineuroinflammatory activity.

EXPERIMENTAL SECTION

General Experimental Procedures. The experimental procedures were performed as previously described.¹⁷

Plant Material. The twigs of *P. koraiensis* were obtained from Hongcheon, Korea, in May 2016, and the plant was authenticated by one of the authors (K.R.L.). A voucher specimen (SKKU-NPL 1414) of the plant is deposited at the herbarium of the School of Pharmacy, Sungkyunkwan University, Suwon, Korea.

Extraction and Isolation. *P. koraiensis* (10.0 kg) twigs were extracted three times with 80% aqueous MeOH under reflux and filtered. The residue was concentrated under reduced pressure to obtain a MeOH extract (665 g). The crude extract was suspended in distilled water and partitioned with *n*-hexane, CHCl₃, EtOAc, and *n*-BuOH, yielding 39, 50, 22, and 65 g of residue, respectively. The EtOAc-soluble fraction (22 g) was separated on a silica gel column (CHCl₃–MeOH–H₂O, 7:1:0.1 \rightarrow 1:1:0.1) to yield eight fractions (E1–E8). Fraction E2 (3.7 g) was separated on an RP-C₁₈ silica gel column, eluting with 35% aqueous MeOH, to acquire eight subfractions (E2A–E2H). Subfraction E2G (440 mg) was purified by C₁₈ semipreparative HPLC (2 mL/min, 32% aqueous CH₃CN) to obtain compounds 12 (*t*_R: 40.3 min, 136 mg) and 13 (*t*_R: 49.0 min, 18 mg). Fraction E4 (2.8 g) was chromatographed on an RP-C₁₈ silica gel column with 30% aqueous MeOH to give 11 subfractions (E4A–E4K). Subfraction E4E (338 mg) was subjected to a LiChroprep Lobar-A Si gel 60 column (CHCl₃–MeOH, 10:1) to acquire three subfractions (E4E1–E4E3). Subfraction E4E3 (126 mg) was purified by semipreparative HPLC (2 mL/min, 21% aqueous CH₃CN) to afford compound 3 (*t*_R: 35.3 min, 22 mg). Compounds 4 (*t*_R: 52.2 min, 3 mg), 6 (*t*_R: 54.1 min, 3 mg), 7 (*t*_R: 60.4 min, 5 mg), and 11 (*t*_R: 69.1 min, 3 mg) were obtained from fraction E4F (172 mg) using a LiChroprep Lobar-A Si gel 60 column (CHCl₃–MeOH–H₂O, 6.5:1:0.1) followed by semipreparative HPLC (2 mL/min, 22% aqueous CH₃CN). Subfraction E4G (208 mg) was separated on a LiChroprep Lobar-A Si gel 60 column (CHCl₃–MeOH–H₂O, 6:1:0.1), followed by semipreparative HPLC (26% aqueous MeOH), to obtain compound 5 (*t*_R: 35.1 min, 4 mg). Using a LiChroprep Lobar-A Si gel 60 column with CHCl₃–MeOH (10:1), subfraction E4I (319 mg) was fractionated into three further subfractions (E4I1–E4I3). Subfraction E4I3 (117 mg) was purified by semipreparative HPLC (29% aqueous CH₃CN) to afford compounds 1 (*t*_R: 32.1 min, 2 mg), 2 (*t*_R: 33.4 min, 5 mg), and 8 (*t*_R: 50.2 min, 20 mg). Fraction E6 (3.8 g) was subjected to an RP-C₁₈ silica gel column with 35% aqueous MeOH to obtain 12 subfractions (E6A–E6L). Subfraction E6I (607 mg) was separated on a silica gel column (CHCl₃–MeOH–H₂O, 4:1:0.1) to yield two subfractions (E6I1 and E6I2). Subfraction E6I1 (220 mg) was isolated by semipreparative HPLC (57% aqueous MeOH) to obtain compounds 9 (*t*_R: 22.7 min, 10 mg) and 10 (*t*_R: 24.3 min, 2 mg).

Koraienside A (1): colorless gum; [α]_D²⁵ +62 (*c* 0.1, MeOH); ECD (MeOH) λ _{max} ($\Delta\epsilon$) 225 (+2.45) nm; IR (KBr) ν _{max} 3864, 3627, 3551, 2973, 2869, 1639, 1409, 1051 cm⁻¹; ¹H (700 MHz) and ¹³C (175 MHz) NMR data in methanol-*d*₄, see Tables 1 and 2; HRESIMS (positive-ion mode) *m/z* 535.2516 [M + Na]⁺ (calcd for C₂₆H₄₀O₁₀Na, 535.2519).

Koraienside B (2): colorless gum; [α]_D²⁵ +28 (*c* 0.1, MeOH); UV (MeOH) λ _{max} (log ϵ) 218 (2.11) nm; ECD (MeOH) λ _{max} ($\Delta\epsilon$) 225 (+3.11) nm; IR (KBr) ν _{max} 3552, 3160, 2975, 2869, 2358, 1644, 1404, 1053 cm⁻¹; ¹H (700 MHz) and ¹³C (175 MHz) NMR data in

methanol- d_4 , see Tables 1 and 2; HRESIMS (positive-ion mode) m/z 535.2520 $[M + Na]^+$ (calcd for $C_{26}H_{40}O_{10}Na$, 535.2519).

Koraienside C (3): colorless gum; $[\alpha]_D^{25} +22$ (c 0.1, MeOH); UV (MeOH) λ_{max} (log ϵ) 218 (1.90) nm; ECD (MeOH) λ_{max} ($\Delta\epsilon$) 227 (+2.67) nm; IR (KBr) ν_{max} 3550, 3172, 1660, 1398, 1053 cm^{-1} ; 1H (700 MHz) and ^{13}C (175 MHz) NMR data in methanol- d_4 , see Tables 1 and 2; HRESIMS (positive-ion mode) m/z 535.2467 $[M + Na]^+$ (calcd for $C_{26}H_{40}O_{10}Na$, 535.2519).

Koraienside D (4): colorless gum; $[\alpha]_D^{25} +12$ (c 0.1, MeOH); UV (MeOH) λ_{max} (log ϵ) 220 (1.82) nm; ECD (MeOH) λ_{max} ($\Delta\epsilon$) 224 (+2.43) nm; IR (KBr) ν_{max} 3553, 3481, 3194, 1654, 1402, 1054 cm^{-1} ; 1H (700 MHz) and ^{13}C (175 MHz) NMR data in methanol- d_4 , see Tables 1 and 2; HRESIMS (positive-ion mode) m/z 533.2363 $[M + Na]^+$ (calcd for $C_{26}H_{38}O_{10}Na$, 533.2363).

Koraienside E (5): colorless gum; $[\alpha]_D^{25} +2$ (c 0.1, MeOH); UV (MeOH) λ_{max} (log ϵ) 217 (2.01) nm; ECD (MeOH) λ_{max} ($\Delta\epsilon$) 225 (+2.97) nm; IR (KBr) ν_{max} 3678, 3602, 2974, 2869, 2350, 1643, 1338, 1054 cm^{-1} ; 1H (700 MHz) and ^{13}C (175 MHz) NMR data in methanol- d_4 , see Tables 1 and 2; HRESIMS (positive-ion mode) m/z 533.2366 $[M + Na]^+$ (calcd for $C_{26}H_{38}O_{10}Na$, 533.2363).

Koraienside F (6): colorless gum; $[\alpha]_D^{25} +16$ (c 0.1, MeOH); UV (MeOH) λ_{max} (log ϵ) 217 (2.34) nm; ECD (MeOH) λ_{max} ($\Delta\epsilon$) 220 (+1.40) nm; IR (KBr) ν_{max} 3553, 3152, 2971, 2837, 1653, 1408, 1040 cm^{-1} ; 1H (700 MHz) and ^{13}C (175 MHz) NMR data in methanol- d_4 , see Tables 1 and 2; HRESIMS (positive-ion mode) m/z 533.2365 $[M + Na]^+$ (calcd for $C_{26}H_{38}O_{10}Na$, 533.2363).

Koraienside G (7): colorless gum; $[\alpha]_D^{25} +26$ (c 0.1, MeOH); UV (MeOH) λ_{max} (log ϵ) 219 (1.88) nm; ECD (MeOH) λ_{max} ($\Delta\epsilon$) 225 (+2.13) nm; IR (KBr) ν_{max} 3662, 3513, 2972, 2836, 1653, 1410, 1042 cm^{-1} ; 1H (700 MHz) and ^{13}C (175 MHz) NMR data in methanol- d_4 , see Tables 1 and 2; HRESIMS (positive-ion mode) m/z 533.2363 $[M + Na]^+$ (calcd for $C_{26}H_{38}O_{10}Na$, 533.2363).

Koraienside H (8): colorless gum; $[\alpha]_D^{25} +4$ (c 0.1, MeOH); UV (MeOH) λ_{max} (log ϵ) 217 (1.51) nm; ECD (MeOH) λ_{max} ($\Delta\epsilon$) 226 (+3.01) nm; IR (KBr) ν_{max} 3719, 3601, 3164, 2972, 2869, 1648, 1406, 1053 cm^{-1} ; 1H (700 MHz) and ^{13}C (175 MHz) NMR data in methanol- d_4 , see Tables 1 and 2; HRESIMS (positive-ion mode) m/z 649.2832 $[M + Na]^+$ (calcd for $C_{31}H_{46}O_{13}Na$, 649.2836).

Koraienside I (9): colorless gum; $[\alpha]_D^{25} +16$ (c 0.1, MeOH); ECD (MeOH) λ_{max} ($\Delta\epsilon$) 222 (+2.11) nm; IR (KBr) ν_{max} 3720, 3588, 3511, 3178, 2973, 2869, 1340, 1053 cm^{-1} ; 1H (700 MHz) and ^{13}C (175 MHz) NMR data in methanol- d_4 , see Tables 1 and 2; HRESIMS (positive-ion mode) m/z 521.2725 $[M + Na]^+$ (calcd for $C_{26}H_{42}O_9Na$, 521.2727).

Koraienside J (10): colorless gum; $[\alpha]_D^{25} +3$ (c 0.1, MeOH); ECD (MeOH) λ_{max} ($\Delta\epsilon$) 223 (+1.87) nm; IR (KBr) ν_{max} 3681, 3600, 3552, 3511, 2973, 2869, 2073, 1407, 1053 cm^{-1} ; 1H (700 MHz) and ^{13}C (175 MHz) NMR data in methanol- d_4 , see Tables 1 and 2; HRESIMS (positive-ion mode) m/z 521.2728 $[M + Na]^+$ (calcd for $C_{26}H_{42}O_9Na$, 521.2727).

Koraienside K (11): colorless gum; $[\alpha]_D^{25} +15$ (c 0.1, MeOH); UV (MeOH) λ_{max} (log ϵ) 221 (2.43) nm; ECD (MeOH) λ_{max} ($\Delta\epsilon$) 225 (+1.35) nm; IR (KBr) ν_{max} 3552, 3516, 3162, 2989, 2841, 1652, 1408, 1043 cm^{-1} ; 1H (700 MHz) and ^{13}C (175 MHz) NMR data in methanol- d_4 , see Tables 1 and 2; HRESIMS (positive-ion mode) m/z 519.2208 $[M + Na]^+$ (calcd for $C_{25}H_{36}O_{10}Na$, 519.2206).

Computational Analysis. Information regarding the DP4+ and ECD calculations are provided in the Supporting Information.

Enzymatic Hydrolysis of Compounds 1–11. A solution of each sample (0.5–1.0 mg) in H_2O (1.0 mL) was individually hydrolyzed with β -glucosidase (10 mg, from almonds, Sigma-Aldrich, St. Louis, MO, USA) at 37 °C for 48 h. After hydrolysis, each reaction mixture was extracted with $CHCl_3$ to obtain aglycones 1a–6a and 8a–10a (0.3–0.5 mg).

13 α -Hydroxy-8(17)-labden-(15→16)-lacton-19-oic acid (1a): colorless gum; $[\alpha]_D^{25} +103$ (c 0.1, MeOH); ECD (MeOH) λ_{max} ($\Delta\epsilon$) 222 (+0.27) nm; 1H (700 MHz) and ^{13}C (175 MHz) NMR data in methanol- d_4 , see Tables S6 and S7, Supporting Information; HRESIMS (positive-ion mode) m/z 373.1989 $[M + Na]^+$ (calcd for $C_{20}H_{30}O_5Na$, 373.1991).

8 β -Hydroxylabd-13-en-(15→16)-lacton-19-oic acid (2a): colorless gum; $[\alpha]_D^{25} +117$ (c 0.1, MeOH); UV (MeOH) λ_{max} (log ϵ) 218 (1.31) nm; ECD (MeOH) λ_{max} ($\Delta\epsilon$) 218 (+0.71) nm; 1H (700 MHz) and ^{13}C (175 MHz) NMR data in methanol- d_4 , see Tables S6 and S7, Supporting Information; HRESIMS (positive-ion mode) m/z 373.1990 $[M + Na]^+$ (calcd for $C_{20}H_{30}O_5Na$, 373.1991).

8 α -Hydroxylabd-13-en-(15→16)-lacton-19-oic acid (3a): colorless gum; $[\alpha]_D^{25} +11$ (c 0.1, MeOH); UV (MeOH) λ_{max} (log ϵ) 218 (1.28) nm; ECD (MeOH) λ_{max} ($\Delta\epsilon$) 227 (+1.20) nm; 1H (700 MHz) and ^{13}C (175 MHz) NMR data in methanol- d_4 , see Tables S6 and S7, Supporting Information; HRESIMS (positive-ion mode) m/z 373.1990 $[M + Na]^+$ (calcd for $C_{20}H_{30}O_5Na$, 373.1991).

17-Hydroxylabda-7,13-diene-(15→16)-lacton-19-oic acid (4a): colorless gum; $[\alpha]_D^{25} +16$ (c 0.1, MeOH); UV (MeOH) λ_{max} (log ϵ) 220 (1.33) nm; ECD (MeOH) λ_{max} ($\Delta\epsilon$) 224 (+0.67) nm; 1H (700 MHz) and ^{13}C (175 MHz) NMR data in methanol- d_4 , see Tables S6 and S7, Supporting Information; HRESIMS (positive-ion mode) m/z 371.1834 $[M + Na]^+$ (calcd for $C_{20}H_{28}O_5Na$, 371.1834).

3 β -Hydroxylabda-8(17),13-diene-(15→16)-lacton-19-oic acid (5a): colorless gum; $[\alpha]_D^{25} +91$ (c 0.1, MeOH); UV (MeOH) λ_{max} (log ϵ) 217 (1.10) nm; ECD (MeOH) λ_{max} ($\Delta\epsilon$) 220 (+1.43) nm; 1H (700 MHz) and ^{13}C (175 MHz) NMR data in methanol- d_4 , see Tables S6 and S7, Supporting Information; HRESIMS (positive-ion mode) m/z 371.1836 $[M + Na]^+$ (calcd for $C_{20}H_{28}O_5Na$, 371.1834).

3 α -Hydroxylabda-8(17),13-diene-(15→16)-lacton-19-oic acid (6a): colorless gum; $[\alpha]_D^{25} +75$ (c 0.1, MeOH); UV (MeOH) λ_{max} (log ϵ) 217 (1.21) nm; ECD (MeOH) λ_{max} ($\Delta\epsilon$) 220 (+0.81) nm; 1H (700 MHz) and ^{13}C (175 MHz) NMR data in methanol- d_4 , see Tables S6 and S7, Supporting Information; HRESIMS (positive-ion mode) m/z 371.1835 $[M + Na]^+$ (calcd for $C_{20}H_{28}O_5Na$, 371.1834).

Pinusolidic acid (8a): colorless gum; $[\alpha]_D^{25} +45$ (c 0.1, MeOH); UV (MeOH) λ_{max} (log ϵ) 217 (1.35) nm; ECD (MeOH) λ_{max} ($\Delta\epsilon$) 222 (+1.33) nm; 1H NMR ($CDCl_3$, 700 MHz) δ 7.10 (1H, brt, $J = 1.4$ Hz, H-14), 4.89 (1H, brs, H-17a), 4.77 (2H, overlap, H-15), 4.59 (1H, brs, H-17b), 1.24 (3H, s, H-18), 0.60 (3H, s, H-20); ESIMS (negative-ion mode) m/z 331.2 $[M - H]^-$.

Labda-8(17),13E-diene-15,16-diol-19-oic acid (9a): colorless gum; $[\alpha]_D^{25} +19$ (c 0.1, MeOH); ECD (MeOH) λ_{max} ($\Delta\epsilon$) 220 (+0.75) nm; 1H (700 MHz) and ^{13}C (175 MHz) NMR data in methanol- d_4 , see Tables S6 and S7, Supporting Information; HRESIMS (positive-ion mode) m/z 359.2197 $[M + Na]^+$ (calcd for $C_{20}H_{32}O_4Na$, 359.2198).

Labda-8(17),13E-diene-15,16-diol-19-oic acid (10a): colorless gum; $[\alpha]_D^{25} +11$ (c 0.1, MeOH); ECD (MeOH) λ_{max} ($\Delta\epsilon$) 224 (+0.51) nm; HRESIMS (positive-ion mode) m/z 359.2198 $[M + Na]^+$ (calcd for $C_{20}H_{32}O_4Na$, 359.2198).

Acid Hydrolysis of Compound 8. Compound 8 (1.0 mg) was refluxed with 1 N HCl (1.0 mL) for 2 h at 90 °C. The hydrolysate was diluted with H_2O and extracted with $CHCl_3$. The aqueous layer was neutralized by passing through an Amberlite IRA-67 column to obtain the sugar. The organic layer was concentrated under reduced pressure to yield 8b.

Labda-8,13-dien-16,15-olid-19-oic acid (8b): colorless gum; 1H NMR (methanol- d_4 , 700 MHz) δ 7.39 (1H, brt, $J = 1.5$ Hz, H-14), 4.84 (2H, overlap, H-15), 1.68 (3H, s, H-17), 1.24 (3H, s, H-18), 0.94 (3H, s, H-20); ESIMS (negative-ion mode) m/z 331.2 $[M - H]^-$.

Determination of Absolute Configuration of Sugar Moieties of Compounds 1–11. The experimental procedures were performed as previously described.¹⁶ D-Glucose and L-arabinose were identified by co-injection with standard silylated samples, giving a single peak at 11.468 min (D-glucose) and 9.312 min (L-arabinose). Authentic samples (Sigma-Aldrich, St. Louis, MO, USA) treated in the same way showed a single peak at 11.467 min (D-glucose) and 9.320 min (L-arabinose), respectively.

NGF and Cell Viability Assays and NO Production and Viability in LPS-Stressed BV2 Cells. The bioactivity assays were performed using the methods reported previously.¹⁷

■ ASSOCIATED CONTENT**SI Supporting Information**

The Supporting Information is available free of charge at <https://pubs.acs.org/doi/10.1021/acs.jnatprod.9b01158>.

HRESIMS and NMR data of compounds **1–11**, **1a–6a**, and **9a**, HRESIMS data of **10a**, and computational data (PDF)

■ AUTHOR INFORMATION**Corresponding Author**

Kang Ro Lee – Natural Products Laboratory, School of Pharmacy, Sungkyunkwan University, Suwon 16419, Republic of Korea; orcid.org/0000-0002-3725-5192; Phone: +82-31-290-7710; Email: krlee@skku.edu; Fax: +82-31-290-7730

Authors

Kyoung Jin Park – Natural Products Laboratory, School of Pharmacy, Sungkyunkwan University, Suwon 16419, Republic of Korea

Zahra Khan – College of Pharmacy and Gachon Institute of Pharmaceutical Science, Gachon University, Incheon 21936, Republic of Korea

Lalita Subedi – College of Pharmacy and Gachon Institute of Pharmaceutical Science, Gachon University, Incheon 21936, Republic of Korea

Sun Yeou Kim – College of Pharmacy and Gachon Institute of Pharmaceutical Science, Gachon University, Incheon 21936, Republic of Korea

Complete contact information is available at:

<https://pubs.acs.org/10.1021/acs.jnatprod.9b01158>

Notes

The authors declare no competing financial interest.

■ ACKNOWLEDGMENTS

This research was supported by the Basic Science Research Program through the National Research Foundation of Korea (NRF), funded by the Ministry of Education, Science and Technology (2016R1A2B2008380). We are grateful to the Korea Basic Science Institute (KBSI) for the mass spectrometric analysis.

■ REFERENCES

- (1) McAllister, A. K. *Cell. Mol. Life Sci.* **2001**, *58*, 1054–1060.
- (2) Dawbarn, D.; Allen, S. J. *Neuropathol. Appl. Neurobiol.* **2003**, *29*, 211–230.
- (3) Amor, S.; Puentes, F.; Baker, D.; van der Valk, P. *Immunology* **2010**, *129*, 154–169.
- (4) Block, M. L.; Zecca, L.; Hong, J. S. *Nat. Rev. Neurosci.* **2007**, *8*, 57–69.
- (5) Lee, T. K.; Park, J. Y.; Yu, J. S.; Jang, T. S.; Oh, S. T.; Pang, C.; Ko, Y. J.; Kang, K. S.; Kim, K. H. *Bioorg. Med. Chem. Lett.* **2018**, *28*, 1084–1089.
- (6) Liang, R.; Cheng, S.; Wang, X. *Food Chem.* **2018**, *254*, 170–184.
- (7) Qu, H.; Gao, X.; Zhao, H. T.; Wang, Z. Y.; Yi, J. J. *Carbohydr. Polym.* **2019**, *223*, 115056.
- (8) Su, X.-Y.; Wang, Z.-Y.; Liu, J.-R. *Food Chem.* **2009**, *117*, 681–686.
- (9) Lee, T. K.; Roh, H.-S.; Yu, J. S.; Baek, J.; Lee, S.; Ra, M.; Kim, S. Y.; Baek, K.-H.; Kim, K. H. *Chem. Biodiversity* **2017**, *14*, e1600400.
- (10) Zhang, H.; Zhao, H.; Zhou, X.; Yang, X.; Shen, S.; Wang, J.; Wang, Z.; Geng, L. *RSC Adv.* **2016**, *6*, 110706–110721.

(11) Wang, L.; Li, X.; Wang, H. *Int. J. Biol. Macromol.* **2019**, *126*, 385–391.

(12) Yi, J.; Cheng, C.; Li, X.; Zhao, H.; Qu, H.; Wang, Z.; Wang, L. *Food Funct.* **2017**, *8*, 151–166.

(13) Chen, L.-X.; Qiu, F.; Wei, H.; Qu, G.-X.; Yao, X.-S. *Helv. Chim. Acta* **2006**, *89*, 2654–2664.

(14) Waridel, P.; Wolfender, J. L.; Lachavanne, J. B.; Hostettmann, K. *Phytochemistry* **2004**, *65*, 945–954.

(15) Wu, L. B.; Xiao, C. J.; Jiang, X.; Qiu, L.; Dong, X.; Jiang, B. *Chem. Biodiversity* **2015**, *12*, 1229–1236.

(16) Kim, C. S.; Subedi, L.; Park, K. J.; Kim, S. Y.; Choi, S. U.; Kim, K. H.; Lee, K. R. *Fitoterapia* **2015**, *106*, 147–152.

(17) Park, K. J.; Kim, C. S.; Khan, Z.; Oh, J.; Kim, S. Y.; Choi, S. U.; Lee, K. R. *J. Nat. Prod.* **2019**, *82*, 1345–1353.

(18) Hara, S.; Okabe, H.; Mihashi, K. *Chem. Pharm. Bull.* **1987**, *35*, 501–506.

(19) Hu, C.-L.; Xiong, J.; Wang, P.-P.; Ma, G.-L.; Tang, Y.; Yang, G.-X.; Li, J.; Hu, J.-F. *Phytochem. Lett.* **2017**, *20*, 239–245.

(20) Suh, W. S.; Kim, K. H.; Kim, H. K.; Choi, S. U.; Lee, K. R. *Helv. Chim. Acta* **2015**, *98*, 1087–1094.

(21) Chiang, Y.-M.; Liu, H.-K.; Lo, J.-M.; Chien, S.-C.; Chan, Y.-F.; Lee, T.-H.; Su, J.-K.; Kuo, Y.-H. *J. Chin. Chem. Soc.* **2003**, *50*, 161–166.

(22) Shen, Y. H.; Li, R. T.; Xiao, W. L.; Xu, G.; Lin, Z. W.; Zhao, Q. S.; Sun, H. D. *J. Nat. Prod.* **2006**, *69*, 319–322.

(23) Quon, H. H.; Swan, E. P. *Can. J. Chem.* **1969**, *47*, 4389–4392.

(24) Bohlmann, F.; Suding, H.; Cuatrecasas, J.; King, R. M.; Robinson, H. *Phytochemistry* **1980**, *19*, 267–271.

(25) Jung, H. A.; Lee, E. J.; Kim, J. S.; Kang, S. S.; Lee, J.-H.; Min, B.-S.; Choi, J. S. *Arch. Pharmacol. Res.* **2009**, *32*, 1399–1408.

(26) Pristovšek, P.; Franzoni, L. *J. Comput. Chem.* **2006**, *27*, 791–797.